Using Ray Tracing for Site-Specific Indoor Radio Signal Strength Analysis

Article · January 1996

Source: CiteSeer

1 author:

Michael Nidd
IBM

Using Ray Tracing for Site-Specific Indoor Radio Signal Strength Analysis [1]

Michael Nidd, Stephen Mann, and Jay Black
Computer Science Department, University of Waterloo, Waterloo, Ontario, N2L 3G1, Canada

Abstract

A variation of cone-tracing is used to predict the signal strength in wireless networks. Differences between light and radio waves necessitate certain changes to the basic ray/cone tracing algorithm, as does the information required of the solution. The new algorithm is compared to a previous algorithm for signal strength prediction, and verified on some examples.

I. Introduction

Cellular radio is a victim of its own success. As more uses are found for the fixed bandwidth available in the electromagnetic spectrum, the availability of that bandwidth is decreasing. The only extensible solution is to decrease the transmission area used by a single device, meaning lower power transmissions and smaller cells. When the transmission power is low, it is important to make the most of the available coverage. This means that care must be taken when placing antennas to minimize both the area of poor coverage and the overlap between different antennas' regions. In this paper, we present a technique for analyzing signal strength in a room or set of rooms.

Radio waves are similar to light waves, just at a much lower frequency. Although the rules for reflection, refraction, and scattering are similar for both types of waves, the longer waves in radio ($\sim$30cm) are significantly different from light in two important respects. First, the systematic interference caused by the coherence of the transmitted waves and the long wavelengths means that the signal strength does not fade uniformly along a line of sight from the transmitter. Second, the interactions between the signal and a surface that is only one or two wavelengths across is no longer the same as for visible light. The first of these difficulties is addressed by the technique presented in this paper. Dealing properly with the second problem requires an exact solution, which is more complicated and time-consuming [10]. In this paper we avoid this second problem by dealing only with objects having planar surfaces at least two meters on each side.

The strength of the transmitted signal depends on the type of transmitter being used, but more important is the drop in signal that the receiver can detect. Common receivers can resolve signals that are 0.1% of the transmitted intensity. Typically, only 10% of the signal strength remains after reflection or transmission, although these number vary widely due to the large variation of materials found in buildings. See the papers by Cox et al. [2, 3] for a range of examples.

Areas of poor coverage are the result of multiple propagation paths existing between the transmitter and a given receiver position. Because these paths have different lengths, the relative phases of the received carrier waves are not predictable. If they are 180 degrees out of phase, then they completely cancel each other out. This is called "multipath interference." When predicting this interference, the optical distance traveled by each component signal must be known to within a fixed tolerance. The difficulty presented by this restriction is that this tolerance does not relax at large distances from the transmitter. In the case of 1GHz waves, a 15cm error in distance will cause the phase to be inverted, resulting in destructive interference being predicted where constructive should have been observed, and vice versa. Because wavelength is constant, that 15cm error causes the same error in phase angle near the antenna as it does far from the antenna.

Previous work on determining signal strength for indoor wireless networks falls into two major categories, statistical methods (see [6]) and site-specific methods. Statistical methods essentially "average" all the objects in the scene, and do not report variations in signal strength around any particular object. While this is useful in describing an average propagation pattern for an antenna (e.g. "X has a range of 20 meters, given line-of-sight, in a factory floor environment.") it does not help the system planner decide how to position the antenna for optimal performance. Most of the site-specific techniques have been variations on ray tracing. For example, Seidel and Rappaport [11, 12, 13] use a ray tracing technique to predict the signal strength at a particular location. However, their technique is limited to predicting the signal strength at a single, one point-receiver. Lecours et al. [5] used a similar ray tracing method that they verified with physical measurements. A paper by McKown and Hamilton [7] also employs ray tracing, but it uses a very different technique for intersecting rays with objects, and for dynamically adjusting the resolution in areas with a high signal strength gradient. The technique closest to that used here has been proposed by Sipilä and Heiska [14]. Their method differs only in the use of a pre-set maximum number of reflected rays, rather than the cone models discussed below. See [9] for a more complete survey of previous work in signal strength prediction.

Ideally, we would be able to predict the signal strength at all points within the room(s) of interest. However, it should be sufficient to predict the signal strength on a single plane in the room (parallel to the floor) because the wireless devices using the network are usually either desktop or handheld, which we expect to be at a roughly constant distance above the floor.

Most of the site-specific techniques only compute the signal strength at a single point, the exceptions being Keenan and Motley [8] and McKown and Hamilton [7]. Keenan and Motley compute the signal strength solely as a function of distance and the number of walls between the source and receiver. McKown and Hamilton calculate the strength at a grid of receiver points, then dynamically increase the resolution of the receiver grid in

[1] This work was supported in part by the Advanced Radiodata Research Center of Motorola Canada Ltd. and the Natural Sciences and Engineering Research Council of Canada

areas of high variability. Their technique is expensive because for each receiver point they reflect in every possible surface to determine all paths to the transmitter.

In this paper, we describe a method for using ray tracing techniques for signal strength prediction. In computer graphics, standard ray tracing [4, p.701] renders a scene by casting rays from the desired viewing location through an imagined video display. This technique requires the eye-point, display location, resolution, and orientation to be defined a priori, thereby determining the initial rays. The color of the pixel through which each ray passes is determined by casting rays from the nearest intersected surface to all light sources. In a room-sized environment, the physical properties of visible frequency radiation are fairly simple. However, several important differences are encountered when translating this style approach to a radio-frequency environment. First, we are interested in the signal strength at a particular plane in the room. Although similar to the projection plane of ray tracing, for signal strength analysis we are interested in all signals passing through this plane, regardless of the direction of propagation. Second, we are interested in the phase of the waves at each point, as there will be both constructive and destructive interference of these waves. These two differences require us to trace all signals emitted from the source until their strength has attenuated below a given tolerance.

The solution we propose gives an approximation of signal strength for a particular altitude throughout a room. The plane for which the signal is approximated is a collection of discrete squares, which we call the signal intensity grid. The approximation technique first divides the radiated signal into a collection of cones with triangular cross-sections that originate from a single common point, and completely span three-space without overlap. These cones are traced through the room, and reflected off and transmitted through surfaces. We then record the phase and strength of these cones as they pass through the signal intensity grid.

Identifying similarly behaved volumes allows the effect of incident signals to be more efficiently recorded within these areas. If rays are used, care must be taken to avoid having two rays that represent the same optical path from being added to the same discrete area. It is similarly important to avoid having rays straddle a particular area. Using solid cones instead of a dense collections of rays avoids the difficulty of ensuring that each optical path to a discrete portion of a surface is considered exactly once.

II. Cone Tracing

Cone tracing has been used in computer graphics as an anti-aliasing technique for ray tracing [1]. Instead of casting rays, cones are cast into the scene. If the cone partially hits an object, this partial coverage is used to weight the color computed for that cone.

Our use of cones for signal strength prediction differs in that we use the cones to trace the wavefront emitting from a transmitter in all directions. The initial approximation divides the radiated signal into a collection of cones with triangular cross-section that originate from the transmitter, and completely span three-space without overlap.

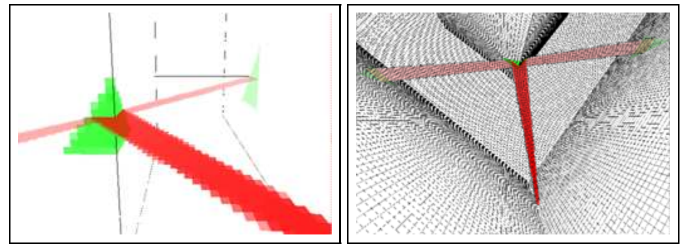

Figure 1: *Cone Tracing. Grid squares in both the signal intensity grid and the various wall panels are filled in darker in areas of stronger radiated intensity (from a single emitted cone).*

Each of these cones can be completely described by three boundary rays and an origin. Each cone is examined to find the closest object intersected by part of the cone. If the entire cone does not strike that object, then the cone is subdivided on the boundaries of the object. Cones that strike exactly one object are used to generate daughter cones corresponding to reflected and transmitted signals. Furthermore, once a cone is seen to be "well behaved," (i.e. it strikes only one wall) its intersection with the signal intensity grid is found, and its effect on this grid is recorded. Fig. 1 gives two different perspective views of this process for a single cone.

A. Phase Calculation

Once a well-behaved cone has been found that intersects exactly one wall, it must be reflected and transmitted. An image of the source (also referred to as a "virtual source") is associated with each cone. The initial location of the virtual source is the actual transmission antenna. Each time the cone is reflected, the source location is also reflected in the plane of the wall (to a point on the other side of the wall having the same perpendicular distance). Thus the straight-line distance to the virtual source is the same as the optical distance to the true source.

If a cone passes through the signal strength intensity grid, its effect on each discrete section of this grid must be found. Both signal strength and phase must be accounted for. As mentioned above, the calculation of optical distance to each of these points must be accurate. Since the current implementation uses only plane reflections, we can use a simple distance calculation ($d^2 = \sqrt{(\Delta x)^2 + (\Delta y)^2 + (\Delta z)^2}$) from each point on the wall to an image of the source.

One problem with this solution is the number of square root calculations involved. One optimization is to calculate the distances to the three corners of the intersection (since the cone is well-behaved, the area of intersection will always be a triangle) and use bilinear interpolation to determine the distances to the intermediate points. This will be faster, but it is less accurate. The inaccuracy results from the fact that the distance between two points does not vary linearly as one point moves in an arbitrary plane. Fig. 2 shows a two-dimensional cross-section of a cone intersecting a wall. In this figure, the distance $\tilde{d}$ is the result of varying the distance from the origin linearly between the two endpoints (i.e. $\tilde{d} = td_1 + (1-t)d_2, 0 \leq t \leq 1$). The maximum error caused by this difference (in the three dimensional case) is bounded by the following [9]:

$$\text{Error} \leq d_{max} \left[3 - 4\sqrt{\frac{1+\cos\gamma}{2}} + \left(\frac{1+\cos\gamma}{2}\right) \right] \quad (1)$$

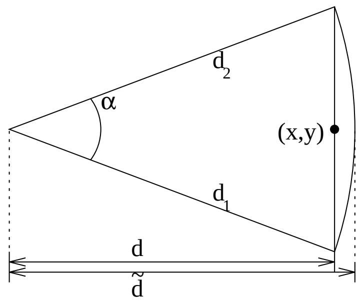

Figure 2: *Cross-section of a cone*

where d_{max} is the maximum distance along any of the three corner rays, and γ is the largest angle between two rays. While this equation still contains a square root, distance is used only as a multiplier. Therefore, the contents of the square brackets above can be calculated ahead of time, and a table lookup can be used at runtime, since the angle of emission is bounded by the largest angle used in sending the initial cone. If the error is too large, then we can subdivide the cones.

B. Subdivision

There are three reasons for subdividing our cones into smaller cones. The first occurs if we are using linear interpolation to simplify the distance calculation and the error is too large. Since the three corners are already known, only one new ray must be traced. This can be done by adding a single ray through the centroid, and recursively examining each of the three cones created by joining an existing edge to this point. Alternatively, one could use either a four-to-one or a two-to-one subdivision of the cones.

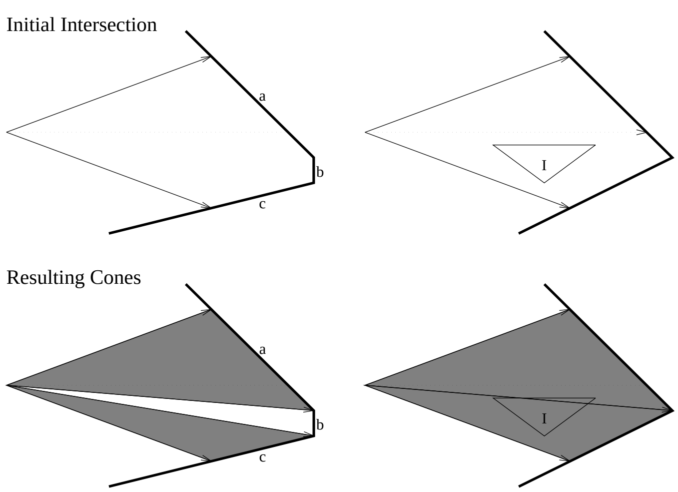

Figure 3: *(left) A wall is missed, but will be detected in the next iteration. (right) A wall is missed, and will not be detected.*

Another reason for subdividing is to prevent the cones from getting so large that they might straddle a wall. Since the current implementation detects interactions with walls only when a corner point intersects one, allowing the edge length to get as large as wall sizes could result in cones passing through walls without having any interaction detected. Because edge length depends on the angle at which the cone is cut, a choice must be made about what should be bounded. We chose to use the lengths of the edges formed when the cone is cut by a plane perpendicular to its direction of propagation, and at a distance equal to the length of the longest edge intersecting a wall (the test is done immediately after determining the intersections of the corner rays).

Since there exists a minimum edge-length for walls, this provides a guideline for choosing a maximum cone size. In practice, 20% of the minimum edge-length has worked well. It should be noted here that pieces of the signal that do not strike the other walls will be detected, as in the left example of Fig. 3. In that case, the portion of the cone that did not strike any of the (up to) three walls detected will be recursively passed back to the tracing function, at which time the new wall will be detected. In the right example of Fig. 3, the whole cone struck parts of the walls that were detected, so there are no remaining fractions to be passed to the next iteration, and the walls that were not detected will remain undetected. However, for our application we do not expect this to occur as we only consider large walls and our limit on the cone size will ensure that all walls are detected.

C. Occlusion

Another difficulty in determining which parts of cones strike walls is the occlusion of one wall by another. The natural solution to this problem is to process the closest wall first, clip on the borders of that wall, and pass the remaining fragments of the cone to the remaining walls. The difficulty with this is the usual problem with occlusion: how to define "closest."

We cast three rays for each cone to find which walls these rays intersect. We then use a variation of the painter's algorithm to determine an ordering on these walls. Details of our variation on the painter's algorithm can be found in [9]. One particular aspect of our method is worth mentioning here. The standard painter's algorithm sorts the polygons based on their distance from the eye-point, using a coordinate system having the eye-point at the origin and with the viewing direction along one axis. However, we will be casting our cones in a large number of directions. We could transform all the polygons to a coordinate system based at the cone's origin, but instead we distinguish "depth" using the cone's origin, a point on each polygon, and the normal to one of the polygons, as illustrated in Fig. 4. This calculation is performed after any required splitting.

III. Results

Lecours et al. [5] developed a simulator based on ray tracing, and published its behavior in both real and imaginary situations. The real situations demonstrated good agreement, and that was presented as an argument that the analysis of imaginary situations also reflected a realistic approximation of the actual signal behavior. As a demonstration of their technique, Lecours et al. generated signal intensity graphs for a single strip of the imaginary room. The reader is referred to the Lecours et al. paper for details of the wall sizes and material properties of this room.

We tested our technique on the Lecours et al. imaginary room. Fig. 5 shows the results of our technique for the portion of this room used in their paper. These are the signal strength predictions for an isotropic radiator one meter from the "front" wall, and one meter below the ceiling. The graphs show the signal strength 2 meters above the floor, along a line one meter from the left wall (the position of this line relative to the room

- Pick a point in each half-plane. Let S be in half-plane 1, P be in half-plane 2, E be the eye point, and N be a normal to half-plane 2
- Iff ((S-E) dot N) * ((P-S) dot N) > 0 then 1 might occlude 2.

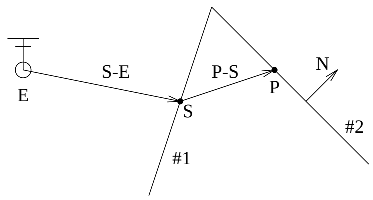

(In this example, #1 might occlude #2.)

Figure 4: *Method for determining possible occlusion between two half planes*

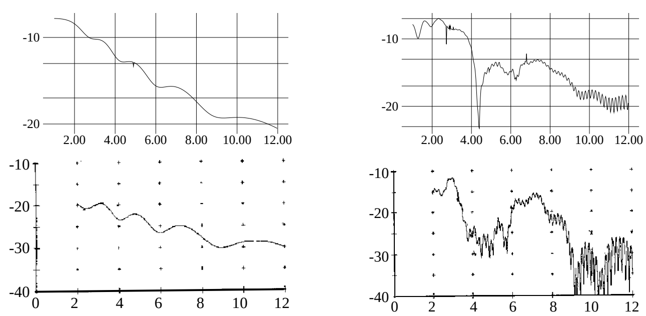

Figure 5: *Cone tracing signal strength for Lecours et al. room. The top row are our simulations. The bottom row are their results*[2]*. The left column simulates the floor only. The right column simulates the complete room. The y-axis gives the signal strength in decibels, and the x-axis is the distance from the back wall. Differences in magnitude are due to antenna gain.*

and transmitter is illustrated Fig. 6). The room is six meters by twelve meters in dimension.

Our results match theirs for the simple case of floor only, and also once the ceiling and side walls are added, in that both sets of results show an area of poor reception in the region from four to six meters along the side wall. In both cases, reception improves in an area six to eight meters along the wall, and the signal quickly degrades after passing the nine meter mark. This latter region (from nine to twelve meters) is strongly influenced by reflections from the end wall, once that wall is added to the model.

While the large-scale behaviors agree between our method and the Lecours et al. method, there is disagreement about the small-scale signal behavior. These differences can be explained by the failure of the current implementation of cone tracing to consider angle of incidence when finding reflection coefficients. The values used were the coefficients for a 45 degree angle of incidence. However, there is actually a significant variation in reflection as a function of incidence angle [12]. This variation accounts for the differences between our results and the results of Lecours et al.

Theoretically, the agreement of the two methods is not a surprise. Although blocks of signal are considered, instead of infinitely thin components, the same reflections are used, so the total interference should be similar. What this experiment shows, however, is that the cone tracing technique can be applied in practice. The graphs in Fig. 5 were generated by a post-analysis loop through one row of the signal strength matrix, and represent only one strip of the room. In fact, by the time they were known, the analysis for the whole room was complete (Fig. 6). This particular analysis took thirty seconds on a lightly loaded RS/6000.

[2]Figures from [5]. Reprinted by author's permission

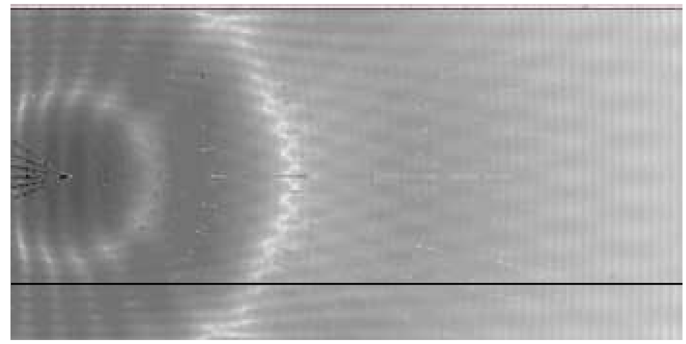

Figure 6: *The signal strength predicted by cone tracing the Lecours et al. room (transmitter is at the left side). Darker areas represent regions of highest signal strength. The black line is the strip used in Fig. 5 and is not part of the signal strength data.*

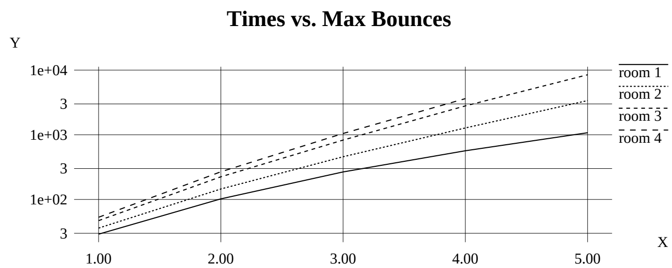

Figure 7: *Execution times for four rooms*

Timings were made for four models. Each room was analyzed for various limits on the number of bounces permitted. Ten trials were performed for each bounce limit in each room, and the averages were used. The user time elapsed was roughly exponential with respect to the bounce limit (Fig. 7). Exponential growth seems natural, since each cone gives birth to some group of daughter cones, and the average number of daughter cones from an incident cone should be independent of the generation numbers of the cones involved.

However, another interesting discovery arising from these trials was how low the bounce limit could be set without significantly affecting the results. The results (shown in Fig. 8) demonstrate that, while the time cost of each step increases, the effect on results decreases. Note that the bounce limit counts only reflections. This allows the weaker signals found in rooms distant from the transmitter to still interfere with each other, even though they may have been severely attenuated by intervening walls.

Combining these results suggests that setting a low limit on

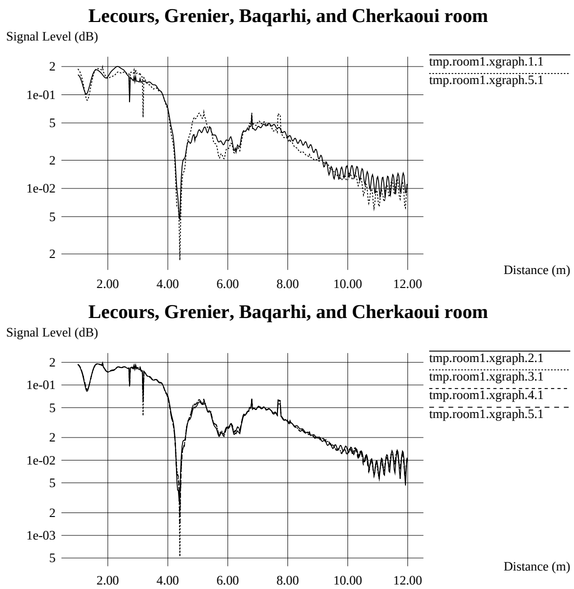

Figure 8: *Bounce limits: The predicted signal strength for the room described in [5] The top graph compares bounce limits of 1 vs. 5, and the bottom shows 2, 3, 4, and 5 together. Note that there is very little qualitative difference between limiting the number of bounces to two, and limiting them to five. Compare this with the execution times shown in Fig. 7.*

the number of bounces will greatly benefit overall efficiency.

IV. Conclusions

This paper has shown an efficient application of cone tracing, which produces useful approximations of signal behavior in specific indoor environments. Using the technique described avoids the mathematical complexities of approximating a solid wavefront with a collection of rays, the redundancies of analyzing the same room for multiple receiver locations, and the inefficiencies of choosing arbitrary initial signal resolutions. It does so by using cones instead of rays, recording signal intensity for the entire room in one pass, and dynamically subdividing cones that become too big.

In addition to many optimizations possible for our current technique (such as computing signal strength for a volume, improving the intersection technique, modeling non-isotropic radiators, etc), there are two interesting effects that could also be modeled. First, surfaces in the presence of an electric field can become secondary emitters. These secondary emissions are uniform in all directions, suggesting that a radiosity technique [4, p.793] could model them effectively. Second, when a wavefront hits a corner or an edge of an object, diffraction effects cause the signal to propagate uniformly from the surface discontinuity. For corners, this results in a spherical wavefront that can be modeled as a new transmitter, but for edges the wavefront will be cylindrical and will require a new model for the signal. A discussion on how to implement these extensions can be found in [9].

References

[1] John Amanatides. Ray tracing with cones. In *Computer Graphics (SIGGRAPH '84 Proceedings)*, pages 129–135, July 1984.

[2] D. C. Cox, R. R. Murray, and A. W. Norris. Measurements of 800 MHz radio transmission into buildings with metallic walls. *The Bell System Technical Journal*, 62(9):2695–2717, November 1983.

[3] D. C. Cox, R. R. Murray, and A. W. Norris. 800 MHz attenuation measured in and around suburban houses. *The Bell System Technical Journal*, 63(6):921–954, July-August 1984.

[4] James D. Foley, Andries van Dam, Steven K. Feiner, and John F. Hughes. *Computer Graphics (second edition)*. Addison-Wesley, 1991.

[5] M. Lecours, D. Grenier, M. Baqarhi, and S. Cherkaoui. Measurements and simulation of received signals in rooms and corridors at 900 MHz and in the 20-60 GHz band. In *43nd annual IEEE Vehicular Technology Conference*, pages 871–874, 1993.

[6] W. C. Lee. *Mobile Communications Engineering*. McGraw Hill, New York, 1982.

[7] John W. McKown and R. Lee Hamilton Jr. Ray tracing as a design tool for radio networks. *IEEE Network Magazine*, pages 27–30, November 1991.

[8] A. Motley and J. Keenan. Personal communication radio coverage in buildings at 900 MHz and 1700 MHz. *Electronics Letters*, 24(12):763–764, June 1988.

[9] Michael Nidd. Using ray tracing for site-specific indoor radio signal strength analysis. Master's thesis, University of Waterloo, Waterloo, Ontario, Canada, 1995.

[10] Keith D. Paulsen, Daniel R. Lynch, and Weiping Liu. Conjugate direction methods for helmholz problems with complex-valued wavenumbers. *International Journal for Numberical Methods in Engineering*, 35:601–622, 1992.

[11] Scott Y. Seidel and Theodore S. Rappaport. A ray tracing technique to predict path loss and delay spread inside buildings. In *Globecom 92*, pages 649–653, 1992.

[12] Scott Y. Seidel and Theodore S. Rappaport. Site-specific propagation prediction for wireless in-building personal communication system design. *IEEE Transactions on Vehicular Technology*, 43(4):879–891, November 1994.

[13] Scott Y. Seidel, Kurt R. Schaubach, Thomas T. Tran, and Theodore S. Rappaport. Research in site-specific propagation modeling for pcs system design. In *43nd annual IEEE Vehicular Technology Conference*, pages 261–264, 1993.

[14] Kari Sipilä and Kari Heiska. Can ray tracing be used as a fading generator in simulating micro-cellular mobile radio systems? In *Wireless 96*, volume 2, pages 538–544, Calgary, Alberta, Canada, July 1996. TRLabs, TRIO, IEEE Canada.